

INSTITUTE FOR FUSION STUDIES

DOE/ER/54346--841

DE-FG03-96ER-54346-841

IFSR #841

Overview of Nonlinear Theory of
Kinetically Driven Instabilities

H.L. BERK AND B.N. BREIZMAN
Institute for Fusion Studies
The University of Texas at Austin
Austin, Texas 78712

September 1998

THE UNIVERSITY OF TEXAS



AUSTIN

MASTER

DISTRIBUTION OF THIS DOCUMENT IS UNLIMITED

DISCLAIMER

This report was prepared as an account of work sponsored by an agency of the United States Government. Neither the United States Government nor any agency thereof, nor any of their employees, make any warranty, express or implied, or assumes any legal liability or responsibility for the accuracy, completeness, or usefulness of any information, apparatus, product, or process disclosed, or represents that its use would not infringe privately owned rights. Reference herein to any specific commercial product, process, or service by trade name, trademark, manufacturer, or otherwise does not necessarily constitute or imply its endorsement, recommendation, or favoring by the United States Government or any agency thereof. The views and opinions of authors expressed herein do not necessarily state or reflect those of the United States Government or any agency thereof.

DISCLAIMER

Portions of this document may be illegible in electronic image products. Images are produced from the best available original document.

Overview of Nonlinear Theory of Kinetically Driven Instabilities

H.L. Berk and B.N. Breizman

Institute for Fusion Studies

The University of Texas at Austin

Austin, Texas 78712

Abstract

An overview is presented of the theory for the nonlinear behavior of instabilities driven by the resonant wave particle interaction. The approach should be applicable to a wide variety of kinetic systems in magnetic fusion devices and accelerators. Here we emphasize application to Alfvén wave driven instability, and the principles of the theory are used to interpret experimental data.

1 Introduction

It has long been realized that the charged fusion products in a fusion-grade plasma (specifically, we treat alpha particles produced by the deuterium-tritium reaction) can potentially destabilize the waves in the plasma [1, 2], and in turn these waves can cause anomalous diffusion of the alpha particles. The instability arises as a result of the wave-particle resonant interaction that taps the free energy of the “universal instability drive” [3] associated with the fast particle pressure gradient.

Among the waves most likely to be excited are so called Toroidal Alfvén Eigenmodes (TAE) [4], whose damping rate in the background plasma is small. This instability has now been observed in many different experiments, where the drive has been due to energetic neutral beams injection [5, 6], ion tails produced by ICRF heating [7]–[9], and alpha particle production by the fusion reaction [10]. An important issue in these experiments is to understand the mode saturation mechanism and the resulting mode spectrum, which often have quite disparate characteristics in different experiments.

To attempt to treat the nonlinear problem, we have developed a basic theory to describe the resonant interaction of particles and waves [11, 12]. This theory applies to a wide variety of systems [13] where instability is driven by the resonant particles. A paradigm model for this study is the excitation of plasma waves due to the bump-on-tail instability, and specific calculations are often performed for this case [11]. However, the formalism readily generalizes to describe the nonlinear behavior of more realistic cases, which include the TAE mode [14], fishbone mode [13], hot electron interchange mode [15], accelerator instabilities [16], etc, where one deals with equations similar to those for the bump-on-tail instability.

An essential feature of our theory, is an emphasis on the single-mode response, where particle sources and collisional relaxation processes are included. We will see that the role of collisions is much stronger than generally appreciated and that we can study [17] the transition between the dynamics associated with a single mode and that associated with the mode overlap regime, described by quasilinear theory. One of the important results of the

theory is the demonstration of different pulsation phenomena, both for single mode [18] and multimode cases [17].

2 Single-Mode Theory

The key ingredient of a general nonlinear theory for the wave-particle interaction is the simplest resonance case, where a longitudinal wave interacts with a free particle of mass m and charge e , in a system without external fields. The particle equation of motion takes the form,

$$\frac{d^2\xi}{dt^2} + \omega_b^2 \sin \xi = 0 \quad (1)$$

where $\xi = \mathbf{k} \cdot \mathbf{r} - \omega t$, $\omega_b^2 = ek \cdot \hat{\mathbf{E}}/m$, and the electric field is given by $\mathbf{E} = \hat{\mathbf{E}} \sin \xi$. Equation (1) can be viewed as that of a pendulum, where ω_b is the small amplitude trapping frequency in the field of the mode.

Indeed, if the wave amplitude is sufficiently small, so that resonances do not overlap, the general resonant wave-particle interaction can be reduced to this form [19]. Specifically, we consider particles in a tokamak, where the unperturbed constants of motion are the energy H , the canonical momentum P_ϕ , and the magnetic moment μ , and the perturbed field depends on time t and azimuthal angle ϕ primarily through the dependence, $n\phi - \int^t \omega dt'$ with n an integer. Then for low frequency waves compared to the cyclotron frequency, the particles respond with μ constant and the energy and canonical momentum constrained to satisfy the relation $dH/dP_\phi = \omega/n$ (thus if ω does not change, it is sufficiently accurate to take $H' = H - \omega P_\phi/n$ as constant in the perturbed fields). The remaining dynamics has been reduced to Eq. (1) [12], where,

$$\omega_b^2 = |n \langle e\mathbf{E} \cdot \mathbf{v} \partial \Omega_p / \partial P_\phi |_{H'} \rangle / \omega|, \quad (2)$$

with $\langle \dots \rangle$ denoting the time average over unperturbed orbits of a particle that satisfies the resonance condition, $\omega = n\omega_\phi - p\omega_\theta \equiv \Omega = d\xi/dt$, with ω_ϕ the averaged unperturbed toroidal drift frequency and ω_θ the unperturbed poloidal bounce frequency with p an integer. Thus the three dimensional dynamics has been reduced to one-dimensional dynamics, or

equivalently the six-dimensional phase space is reduced to two-dimensional phase space. Collisions can also be included by projecting [20] the Fokker-Planck equation upon the phase space "plane" being considered in the dynamics. Thus a Fokker-Planck operator of the form of $\partial/\partial\mathbf{v} \cdot \mathbf{D}(\mathbf{v}) \cdot \partial/\partial\mathbf{v}$, is approximated by the relation $\frac{\partial}{\partial\Omega_p} \nu_{\text{eff}}^3 \frac{\partial}{\partial\Omega_p}$, where $\nu_{\text{eff}}^3 = \langle \partial\Omega_p/\partial\mathbf{v} \cdot \mathbf{D}(\mathbf{v}) \cdot \partial\Omega_p/\partial\mathbf{v} \rangle$ and $\partial\Omega_p/\partial\mathbf{v}$ is evaluated at constant μ and H' . Henceforth we neglect the subscript p in Ω_p . As a result the kinetic equation takes the form,

$$\frac{\partial f}{\partial t} + \Omega \frac{\partial f}{\partial \xi} - \omega_b^2 \sin \xi \frac{\partial f}{\partial \Omega} - \frac{\partial}{\partial \Omega} \nu_{\text{eff}}^3 \frac{\partial f}{\partial \Omega} = 0, \quad (3)$$

with the boundary condition that $\partial f/\partial\Omega$ is unperturbed far from resonance. In effect this boundary condition forces the distribution function to match the solution of the classical transport problem away from the resonance regions.

This kinetic equation has to be solved simultaneously with the equation for the mode evolution. In many problems the mode's spatial structure is known to lowest order. This is the case when the resonant particles can be treated as a perturbation to an eigenmode of the plasma, or the mode structure is determined by a zero frequency constraint, as is the case for the internal kink mode in a tokamak. Then the wave evolution reduces to an equation for each mode amplitude. Typically this equation takes the form,

$$\frac{dA}{dt} + \gamma_d A = e^{i\omega_0 t} \int d\mathbf{r} \mathbf{e}^*(\mathbf{r}, \omega_0) \cdot \mathbf{J}_R(\mathbf{r}, t) \quad (4)$$

where $\mathbf{J}_R(\mathbf{r}, t)$ is the current from the energetic particles and $\text{Re } A(t) \mathbf{e}^*(\mathbf{r}, \omega_0) e^{i\omega_0 t}$ is the perturbed electric field. In this equation we have included linear dissipation that is present in the system even in the absence of energetic particles, and the magnitude of the amplitude, $|A|$ is chosen so that it is the square of the wave trapping frequency, ω_b^2 , of a reference resonant particle that is typical of the system. A somewhat modified wave equation has been derived in Ref. [21], where the left hand side of Eq. (4), describes the linear internal kink mode dynamics with a temporally nonlocal kernel, while the right-hand side is the same as Eq. (4).

Equations (3) and (4) determine the reduced dynamics of the system. When the kinetic contribution is destabilizing, they describe: (1) the competition between the inverse Lan-

dau damping that destabilizes the wave in a plasma and the background damping of the wave due to various nonideal processes; (2) the dominant nonlinearity that arises from the wave-particle resonance interaction; (3) the effects of particle sources and stochastic relaxation processes (e.g. collisions, rf heating, etc.); which are frequently neglected but are more important in the nonlinear theory than in linear theory.

These equations have been studied analytically and have been the basis of numerical simulation [14, 22]. We have found that depending on the strength of the relaxation rate, ν_{eff} , both steady state and pulsating solutions arise in the single mode theory [12, 18]. Extensive analytic insight into the nature of the solutions is obtained by solving the equations in two limits. The first case, (a), is the threshold limit where the trapping frequency is small; [12] either $\omega_b/\nu_{\text{eff}} \ll 1$ or $\int \omega_b dt \ll 1$. The second case, (b), is with these inequalities reversed [18].

Case (a) is particularly important when instability first appears. We solve the kinetic equation by perturbation theory in an expansion in either $(\omega_b/\nu_{\text{eff}})^2$ or $\left(\int \omega_b dt\right)^2$ where to the lowest orders we obtain the equilibrium solution from classical transport processes and the standard linearized perturbation response. We iterate twice beyond linear theory, and we finally obtain the following equation for the mode amplitude A ,

$$\frac{dA}{dt} = (\gamma_L - \gamma_d) A - \frac{\gamma_L e^{i\phi}}{2} \int_0^{t/2} d\tau \tau^2 \int_0^{t-2\tau} d\tau_1 \exp\left(-\nu_{\text{eff}}^3 \tau^2 \left(\frac{2\tau}{3} + \tau_1\right)\right) \cdot A(t-\tau)A(t-\tau-\tau_1)A^*(t-2\tau-\tau_1) \quad (5)$$

For simplicity we have only exhibited the equation for a single resonance, however essentially the same equation may involve a sum over several nonoverlapping resonances. The phase ϕ depends on the linear dispersion relation, and is typically small when the energetic particles only slightly perturb the mode frequency.

Equation (5) exhibits steady and time dependent solutions. The various solutions are shown in Fig. 1 as a function of the parameter, $\nu \equiv \nu_{\text{eff}}/(\gamma_L - \gamma_d)$. Figure 1(a) exhibits a steady solution which arises when $\nu \geq 1$. The form of the solution is $A \sim \nu_{\text{eff}}^2 (1 - \gamma_d/\gamma_L)^{1/2}$. Figures 1(b)-1(c) arise for $\nu \simeq 1$, and show increasingly complicated limit cycles, evolving

from regular sideband oscillations in Fig. 1(b) to more complicated oscillations in Fig. 1(c). Finally, if ν is small enough, the solutions of Eq. (5) are found to diverge in time, as shown in Fig. 1(d). In Ref. [12], self-similar solutions to Eq. (5) are discussed where $|A|/\gamma_L^2 \sim 1/[\gamma_L(t_0-t)]^{5/2}$. This divergence as $t \rightarrow t_0$, is also accompanied by rapid side-band frequency shifting as the time of divergence is approached, as is clear in the oscillatory structure of Fig. 1(d).

Observe that the saturation level of the threshold equation tends to be incremental for the nondivergent solutions, i.e. the saturation level is proportional to an increment by which the system exceeds marginal stability. The equation for the divergent solution, where ν_{eff} is negligible, also indicates a dimensionless amplitude, $A/\gamma_L^2 \sim (\gamma/\gamma_L)^{5/2}$, for the first peak that follows the exponentially growing linear phase. This nonlinear solution then evolves into a self-similar explosive solution that continually overshoots as it grows unboundedly in a finite time. The physical reason for the growth is that a finite amplitude wave tends to flatten the distribution at the position of resonance. However, this flattening needs to steepen the distribution somewhere off-resonance. The self-consistent equations allows a small frequency shift that can tap the steeper gradient in the distribution function that in turn enables a faster growth. The process continually feeds itself as the divergent explosive self-similar solution forms.

The validity of the threshold equation fails when A/γ_L^2 approaches unity. To understand the nature of the saturation a numerical code was developed by Petviashvili [23] based on Eqs. (3) and (4) for a single resonance. He found a rather surprising result. The saturation level was indeed found to scale at a "natural" saturation $\omega_b^2/\gamma_L^2 \sim 1$ caused by particle trapping, but the mode amplitude was found to persist a rather long time, with large frequency shifts as shown in Fig. 2. It was not immediately clear what mechanism could maintain this saturation level (we originally expected that the amplitude would decay rather rapidly, on the time scale $1/\gamma_d$, once saturation due to trapping is achieved). The understanding of this evolution can be obtained by analyzing Eqs. (3) and (4) in the limit associated with case (b) $\omega_b/\nu_{\text{eff}} \gg 1$ or $\int \omega_b dt \gg 1$.

The diagnostics of the simulation indicates that the frequency shifts are associated with the formation of phase space vortices in the destabilizing distribution: holes [24]-[26] whose mean velocity increases with time and clumps [27], whose mean velocity decreases with time. This evolution is clearly seen in Fig. 3, which shows the correlation in the time evolution of the frequency spectrum with the movement of valleys and ridges in the spatially averaged distribution function.

Analytically, this structure is obtained by solving Eqs. (3) and (4) for Bernstein, Greene, Kruskal (BGK) modes [28] where the value of the distribution function in the trapping region is equal to the original value of the distribution function at that Ω -value which is equal to original linear frequency of the wave. The distribution function rapidly changes to the ambient one in the vicinity of the separatrix. A consistent BGK solution with arbitrary frequency shift is found with the constraint that $\omega_b^2 \sim \gamma_L^2$. The needed power balance is obtained by noting that if phase space structures move adiabatically, then the passing particles that skim the separatrices interchange their Ω -position with holes and clumps and as a result when a hole goes to larger Ω -values and a clump moves to lower Ω -values, energy must be released. Straightforward calculations give that the power release arising from the frequency sweeping is proportional to $\gamma_L \frac{d(\delta\omega^2)}{dt} \omega_b$ (where $\delta\omega = \omega - \omega_0$) which should be set equal to $\gamma_d \omega_b^4$, a quantity proportional to the power dissipation rate. This power balance, together with $\omega_b \sim \gamma_L$, then determines the frequency shift with time as $\delta\omega \approx \gamma_L (\gamma_d t)^{1/2}$. The dotted curve in Fig. 4 shows this prediction. In the simulation the amplitude ultimately dies due to collisions on the time scale, $T_{\text{col}} \sim \gamma_L^2 / \nu_{\text{eff}}^3$.

To complete the single wave study we note that if the system is sufficiently far above threshold ($\gamma_L - \gamma_d \sim \gamma_L$), there is no frequency sweeping (in numerical simulation it was found that there was no sweeping if $\gamma_d < .4\gamma_L$). Instead we need to look for solutions with ω nearly constant, but still with the assumptions that $\omega_b / \nu_{\text{eff}} \gg 1$ or $\int \omega_b dt \gg 1$.

First we discuss the scaling of a stable steady solution when $\omega_b / \nu_{\text{eff}} \gg 1$. Analytic solutions have been found when $\gamma_d \ll \gamma_L$ [29] and stability requires $\nu_{\text{eff}}^3 \gg \gamma_L^2 \gamma_d$. The physical basis for the result is that in steady state the average slope of the distribution in

the resonance region has to be reduced by a factor of γ_d/γ_L so that the power released by the resonant energetic particles can match the power absorbed by the linear dissipation channels. If there is no wave present, but there was a plateau in the distribution of width $\Omega - \omega \approx \omega_b$, the time it would take to restore the gradient of the distribution function to that of the ambient gradient surrounding the resonance is $t_1 \sim \omega_b^2/\nu_{\text{eff}}^3$. However in a time $1/\omega_b$ the distribution is flattened by the wave. Hence in the trapping region, the slope of the distribution can only be a fraction, $1/(\omega_b t_1) = \nu_{\text{eff}}^3/\omega_b^3$, of the slope of the ambient distribution. Thus the power transfer from the particle distribution to the wave is reduced from the predictions of linear theory by this factor. A power balance between the resonant particle drive and the dissipation arises when $1/\omega_b t_1 = \gamma_d/\gamma_L$, or equivalently $\omega_b^2 \sim (\gamma_L/\gamma_d)^{2/3} \nu_{\text{eff}}^2$. Combining this result with what we found for the near threshold regime, we obtain the following interpolation formula for the saturation level $\omega_b^2 \sim (\gamma_L/\gamma_d)^{2/3} \nu_{\text{eff}}^2 (1 - \gamma_d/\gamma_L)^{1/2}$. This expression requires $\nu_{\text{eff}}^3 > \gamma_d \gamma_L^2 (1 - \gamma_d/\gamma_L)^3$.

However, when $\nu_{\text{eff}}^3 < \gamma_L^2 \gamma_d$, the steady state solution is unstable [18] and the wave will grow to the level where particle trapping will occur within a single linear growth time, so that $\omega_b^2 \sim \gamma_L^2$, whereupon a plateau forms in the resonance region that prevents the free energy of the distribution function from being tapped. Such an amplitude cannot be maintained in steady state, since plateau formation in the resonance region has nearly eliminated the drive, while one can readily determine [18] that the dissipation is greater than energy influx from particles diffusing from the ambient region into the plateau region. Hence the fields will decay on the time scale $1/\gamma_d$, while the distribution function in the resonance region is being reconstituted on a time scale $T \approx \gamma_L^2/\nu_{\text{eff}}^3$. Thus short time bursts of oscillation must arise whose overall cyclic pattern is on the time scale T . This bursting behavior has been observed in particle simulation codes developed by Pekker [11, 14] and is shown in Fig. 5.

3 Experimental Correlations With Theory

Our theoretical model has been used to interpret the saturated and pulsating responses of the Toroidal Alfvén Eigenmode (TAE) observed in TFTR [7, 10] and JET [30]. In Fig. 6(a)

we show the evolution of a TAE spectrum excited in TFTR by energetic ion tails as a result of ICRF heating. The interesting aspect in this figure is that the TAE signal persists at a lower level after the ICRF is suddenly turned off. Our interpretation of this phenomena is that the near steady saturation levels observed prior to and post shut-off are manifestations of the solutions found in Fig. 1(a), where $\nu_{\text{eff}} > \gamma_L - \gamma_d$. The difference in the amplitudes in these cases is related to the effective collision frequency that needs to be used. With ICRF on, particles diffuse in energy (due to the ICRF heating) and in pitch-angle due to Coulomb scattering, with the heating rate of tails larger than the collisional rate. After shut-off only Coulomb scattering remains and steady saturation is achieved at a lower level. In Fig. 6(b) we show the results of a simulation based on Eq. (5) and observe that we reproduce the character of the experimental signal.

In the future it is important to investigate what happens to tail induced TAE's (or any other kinetically driven waves) if ICRF heating is suddenly turned off. Careful observations of the response will give additional credence (or open new questions) to our theoretical picture. It is important to note that when ICRF is turned off, the TAE signal might suddenly increase rather than diminish. This will happen if the collision frequency is small enough, so that an explosive response can be induced. One might then be able to cleanly observe an explosive response leading to phase space structures in the plasma.

Perhaps such responses have already been seen in dramatic frequency sweeping observations made on the Terrella dipole plasma [15] where the hot electron interchange mode is excited, on C-Mod [9], where an excited Alfvén wave doubles its frequency in 10 ms, on TFTR [31] where one observes the formation frequency sweeping excitations co-existing with a stationary TAE spectrum. More detailed theoretical analysis of these effects is needed.

Recently the pitchfork splitting data in JET have been interpreted [30] in terms of the bifurcations observed in Figs. 1(b)-1(c). Here again the TAE modes are excited by ICRF tails, as shown in Fig. 7, where initially sharply defined spectral lines split into several spectral components. This bifurcation has been modeled with the threshold equation assuming the linear growth rate changes slowly and linearly in time. The result of the simulation can

be compared with the experiment (see Fig. 8), and specific plasma parameters, such as the magnitude of the energetic particle drive, can be inferred from the matching.

The predictions of the saturated level using realistic eigenfunctions and collisional models [32] has been incorporated into the NOVA code [33] that is used to analyze TAE instability. The analytical results have been compared with a numerical simulation of alpha particle TAE driven instability that includes a Monte-Carlo description of collisions [34]. As shown in Fig. 9, excellent agreement is found with the time averaged response of the Monte-Carlo code (the code has a pronounced fluctuation level, whereas the analytic theory predicts a stationary response, but this discrepancy may be related to the noise properties of the Monte-Carlo algorithm). The saturation levels in both these calculations are compatible with experimental observations of alpha particle driven instability in TFTR [10], but more work is needed to identify specific waves in the time sequence they arise in the experiment.

4 Multimode Case

In the multimode case, the different resonant particles can be described by separate pendulum equations, as long as the separation of adjacent resonances is greater than the trapping frequency ω_b so that resonances do not overlap. In the opposite limit the resonances are so closely packed that they blend into a continuum and the usual quasilinear equation can be used. The quasilinear equation can be expressed in terms of the ubiquitous trapping frequency ω_b ,

$$\frac{\partial f}{\partial t} - \frac{\partial}{\partial \Omega} D \frac{\partial}{\partial \Omega} f = \nu(F_0 - f) \quad (6)$$

where $D = \sum_j \omega_{bj}^4 Q(\Omega - \omega_j)$, where the Ω -derivative is with H' and μ constant at the resonant position $\Omega = \omega_j$ and in the continuum limit the sum is an integral and $Q(\Omega - \omega_j) = \pi \delta(\Omega - \omega_j)$. We have also included on the right-hand side a source term, νF_0 , and a particle relaxation rate ν , which together simulate transport processes and in absence of waves allow an energetic particle distribution, F_0 , to be established in a time $1/\nu$.

The wave equation is given by,

$$nG_\omega \frac{\partial}{\partial t} \omega_{bj}^4 - \left(\int d\Omega \frac{\partial P_\phi}{\partial \Omega} Q(\Omega - \omega_j) \frac{\partial f}{\partial \Omega} - 2\gamma_d n G_\omega \right) \omega_{bj}^4 = 0 \quad (7)$$

where $WP_j \equiv nG_\omega \omega_{bj}^4$ is the wave angular momentum of the j^{th} mode (also note that $\omega G_\omega \omega_{bj}^4$ is the mode's wave energy) with G_ω an appropriate function that can be calculated from linear theory. Note that the momentum conservation condition $\frac{\partial}{\partial t} \left(\langle P_\phi \rangle + \int dj WP_j \right) = 0$, is satisfied by Eqs. (6) and (7), where $\langle P_\phi \rangle = \int d\Omega P_\phi f$ when $\gamma_d = \nu = 0$.

There is a qualitative difference between the predictions of the quasilinear equation and the single-mode case [35]. In the single-mode case the distribution function is only significantly modified within the separatrix of the trapping region, while hardly altered outside the separatrix. On the other hand the quasilinear theory allows particles to pass through many resonances, to produce global diffusion. The transition between the two extremes, with built in self-consistency between particles and waves, has yet to be rigorously described in a reduced formalism. However, a heuristic model bridging the gap between these two regimes have been formulated [36], which we will briefly describe here.

Suppose we broaden the delta function, so that it's a peaked function with a finite width $\Delta\hat{\Omega}_j$, and with the normalization condition $\int dx Q(x) = \pi$. Our governing quasilinear equations will still be of the form given by Eqs. (6) and (7), with the broadened functions replacing the delta functions in both these equations. Overall momentum balance is still maintained. When the width of each resonance, $\Delta\hat{\Omega}_j$, exceeds the mode separation, the continuum quasilinear equation is reproduced, while if it is less, one obtains a system of equations that qualitatively reproduce many aspects of the single-mode theory when one chooses $\Delta\hat{\Omega}_j = \gamma_j + \omega_{bj} + \nu_{\text{eff}j}^3 / (\omega_{bj}^2 + \nu_{\text{eff}j}^2)$. In this case diffusion only occurs within a resonance width, but not between resonances. However, now as the mode grows, the resonances can eventually overlap when ω_{bj} becomes comparable to the resonance frequency spacing. We can then describe a transition from the nonoverlap to overlap regimes with our discretized quasilinear model.

A consequence of resonance overlap is the onset of global diffusion, rather than diffusion

only in isolated resonance intervals. Even more dramatically, there is a lot more energy converted into wave energy when resonances overlap. In Fig. 10 we see that a staircase distribution forms when there is flattening in the distribution function from N modes that are not quite overlapping, while there is complete flattening of the distribution in the overlapped case. The ratio of the wave energy release between the overlapped case to the barely nonoverlapped case is $\approx N^2$. The dramatic change in the wave energy release between these two cases, where the input parameters are just incrementally different, gives rise to the possibility of large pulsations, that can be described as phase space explosions, during the transition to the overlap regime.

The continuum quasilinear and the discretized quasilinear model give nearly identical solutions if mode overlap is achieved. Then by examining the steady state solution of the continuum quasilinear equation, we can determine if the diffusion coefficient is large enough to be compatible with a steady state quasilinear equation with N discrete modes. If compatibility is not established, then a steady solution is not possible. Instead, we need to look for a solution where there isn't any global diffusion most of the time; instead global diffusion occurs in short pulses.

We first seek a steady solution of Eqs. (6) and (7) with the boundary conditions $f = 0$ at $\Omega = 0$ (corresponding to particle loss at the plasma edge) and $D \partial f / \partial \Omega = 0$ at $\Omega = \Omega_0$ (corresponding to a zero particle loss condition at the axis of the plasma). With the choice of $F_0 = 2\lambda\gamma_L\Omega$, with $\lambda = n G_\omega / \frac{\partial P_\phi}{\partial \Omega}$ (which for simplicity we take as constant), a steady solution is found of the form, $f = 2\lambda\gamma_d\Omega$ and $D = \nu\gamma_L(\Omega_0^2 - \Omega^2)/2\gamma_d$ where we have assumed $\gamma_L \gg \gamma_d$ and $\nu \ll \gamma_d$. Now to establish compatibility of this solution with mode overlap, we note that the diffusion coefficient D is related to ω_b^2 , by $D \approx \omega_b^4 / \Delta\hat{\Omega}$. To have overlap we require $\omega_b > \Delta\hat{\Omega} \approx \Omega_0/N$. Thus we require $\omega_b^4 \sim \frac{\nu\Omega_0^3\gamma_L}{N\gamma_d} > \left(\frac{\Omega_0}{N}\right)^4$ or equivalently $N > \left(\frac{\gamma_d\Omega_0}{\nu\gamma_L}\right)^{1/3}$. If this condition is not satisfied, we must have either pulsations where the conditions for quasilinear theory is satisfied only for a small fraction of the time, or we obtain a benign response of independent single modes where there is no global diffusion and the energetic particle population is nearly the same as the classical transport prediction.

The basic scalings for the different regimes are as follows: (a) If $\gamma_L < \Omega_0/N^3$ the distribution f will approach its maximum value with only benign nonoverlapping pulsations. (b) If $\gamma_L > \Omega_0/N^3 > \gamma_d$, the distribution will build up well above marginal stability to where $\partial f/\partial\Omega \gtrsim \lambda\Omega/N^3$, but it is then metastable and subject to catastrophic collapse, with loss of nearly all the particles, in short time interval. The quasilinear equations can have a mode-overlapped solution with $D > (\Omega_0/N)^3$, where total particle loss occurs in a time less than γ_d^{-1} . It will take a relatively long time, $T_{\text{recovery}} \sim \Omega_0/(\gamma_L N^3 \nu)$, for the distribution to build up to a level where the next pulse of wave and particle loss can occur. (c) If $\Omega_0/(\gamma_d N^3) < 1$, the quasilinear equation with the constraint, $D \geq (\Omega_0/N)^3$, predicts wave evolution with short pulses and a loss with each pulse of a finite, but small fraction of the stored energetic particles. The fraction of particles lost scales as $(\Omega_0/\gamma_d N^3)^{1/2}$, (a small number) during a short turbulent pulse interval $T_{\text{pulse}} \sim N^{3/2}/(\Omega_0 \gamma_d)^{1/2}$, and then a longer recovery time, $T_{\text{recovery}} \sim (\Omega_0 \gamma_d / N^3)^{1/2} / \nu \gamma_L$ is needed before the instability is retriggered. The last two solutions (cases b and c) have pulsation characteristics similar to the heuristic predator-prey model [37, 38], but in the quasilinear equations basic physics principles govern the dynamics.

In experiments on TFTR [5] and D-IIID [6], where rather intense neutral beams are injected to excite TAE modes, pulsed losses of $\sim 10\%$ of the stored energetic particle number have been observed (see Fig. 11) for TFTR data. We believe that the (c) solution of the quasilinear model can be a basis for understanding this loss behavior. However, more detailed work needs to be performed to make quantitative comparisons.

5 Conclusions

We have outlined a theoretical approach for the study of resonant wave-particle interactions that emphasizes: (1) the universality of the analysis which applies to most kinetic systems, (2) the importance of classical transport processes for describing the nonlinear dynamics, (3) the transition between single mode and multimode phenomena. Though we have mostly applied our result to the Alfvén wave interaction with energetic particles, our approach should be applicable to many physical problems, such as the problem of determining the transport

properties of the bulk plasma in a tokamak. Generalizations of the method described may also apply to fluid equations and lead to such applications as describing heat and current transport processes in an RFP, and to describing the dynamics of the internal kink mode in tokamaks.

References

- [1] M.N. Rosenbluth and P.H. Rutherford, *Phys. Rev. Lett.* **34**, 1428 (1975).
- [2] V.S. Belikov, Ya.I. Kolesnichenko, and V.A. Yavorskij, *Nucl. Fusion* **16**, 783 (1976).
- [3] Rudakov, L.I., and R.Z. Sagdeev, *Sov. Phys. Dokl.* **6**, 415 (1961) [original Russian: *Dokl. Akad. Nauk SSR* **138**, 58 (1961)].
- [4] C.Z. Cheng, L. Chen, and M.S. Chance, *Ann. Phys.* **161**, 21 (1985).
- [5] K.L. Wong, *et al.*, *Phys. Rev. Lett.* **66**, 1874 (1991).
- [6] W.W. Heidbrink, E.J. Strait, E. Doyle, and R. Snider, *Nucl. Fusion* **31**, 1635 (1991).
- [7] K.L. Wong, *et al.*, *Phys. Plasmas* **4**, 393 (1997).
- [8] A. Fasoli *et al.*, *Plasma Phys. Control. Fusion* **39**, B287 (1997).
- [9] J. Snipes *et al.*, *Bull. Am. Phys. Soc.* **42**, 2017 (1997).
- [10] R. Nazikian *et al.*, *Phys. Rev. Lett.* **78**, 2976 (1997).
- [11] H.L. Berk, B.N. Breizman, and M.S. Pekker, *Phys. Plasmas* **2**, 3007 (1995).
- [12] H.L. Berk, B.N. Breizman, M.S. Pekker, *Plasma Phys. Rep.* **23**, 778 (1997) [in Russian origin: *Fizika Plazmy* **23**, 842 (1997)].
- [13] B.N. Breizman, *et al.*, *Phys. Plasmas* **4**, 1559 (1997).
- [14] H.L. Berk, B.N. Breizman, and M.S. Pekker, *Nucl. Fusion* **35**, 1713 (1995).
- [15] H.P. Warren and M.E. Mauel, *Phys. Plasmas* **2**, 4185 (1995).
- [16] G.V. Stupakov, B.N. Breizman, and M.S. Pekker, *Phys. Rev. E* **55**, 5976 (1997).
- [17] B.N. Breizman, H.L. Berk, and H. Ye, *Phys. Fluids B* **5**, 3217 (1993).

- [18] H.L. Berk, B.N. Breizman, and H. Ye, *Phys. Rev. Lett.* **68**, 3563 (1992).
- [19] B.V. Chirikov, *Phys. Rep.* **52**, 263 (1970).
- [20] S.T. Belyaev and G.I. Budker, "Boltzmann's equation for electron gas in which collisions are infrequent," in *Plasma Physics and the Problem of Controlled Thermonuclear Reactions*, edited by M.A. Leontovich (Pergamon Press, London, 1959), Vol. 2, p. 431.
- [21] B.N. Breizman, *et al.*, *Phys. Plasmas* **5**, 1559 (1997).
- [22] J. Candy, *et al.*, *Phys. Plasmas* **4**, 2597 (1997).
- [23] H.L. Berk, B.N. Breizman, and N.V. Petviashvili, *Phys. Lett. A* **234**, 213 (1997).
- [24] H.L. Berk, C.E. Nielsen, and K.V. Roberts, *Phys. Fluids* **13**, 980 (1970).
- [25] P.W. Terry, P.H. Diamond, and T.S. Hahn, *Phys. Fluids B* **2**, 2048 (1990).
- [26] M.E. Mauel, *Journal de Physique IV* **7**, C4-307 (1997).
- [27] T.H. Dupree, *Phys. Fluids* **15**, 334 (1972).
- [28] I.B. Bernstein, J.M. Greene, and M.D. Kruskal, *Phys. Rev.* **108**, 546 (1957).
- [29] H.L. Berk and B.N. Breizman, *Phys. Fluids B* **2**, 2246 (1990).
- [30] A. Fasoli, *et al.*, "Nonlinear splitting of fast particle driven Alfvén eigenmodes: Observation and theory," submitted to *Phys. Rev. Lett.* (July, 1998).
- [31] S. Bernabei, *Bull. Am. Phys. Soc.* **42**, 2040 (1997).
- [32] N.N. Gorelenkov, *et al.*, *Bull. Am. Phys. Soc.* **42**, 1931 (1997).
- [33] C.Z. Cheng, *Phys. Rep.* **211**, 1 (1992).
- [34] W. Chen and R. White, *Bull. Am. Phys. Soc.* **42**, 1982 (1997).
- [35] B.N. Breizman, H.L. Berk, and H. Ye, *Phys. Fluids B* **5**, 3217 (1993).

- [36] H.L. Berk, B.N. Breizman, and J. Fitzpatrick, Nucl. Fusion **35**, 1561 (1995).
- [37] W.W. Heidbrink, *et al.*, Phys. Fluids B **5**, 2176 (1993).
- [38] A.C. Coppi and B. Coppi, Phys. Lett. A **218**, 64 (1996).

Figure Captions

1. Various solutions of the threshold equation. (a) $\nu > \nu_{cr} = 2.1$, solutions asymptote to a steady spectrum; (b) for ν slightly less than ν_{cr} , solutions produce mild sideband oscillations; (c) reducing ν further produces more chaotic oscillations; (d) when ν is sufficiently small and explosive unbounded solution emerges.
2. Persistence of mode amplitude after the explosive case saturates. Note frequency shift from original linear mode frequency increases with time.
3. Evolution of phase space structures with shifting frequency spectrum. In (a) the spatially averaged distribution function is plotted as a function of Ω and time, and the depressions correspond to holes and the ridges to clumps. In (b) the intensity as a function of frequency and time is plotted. Note the precise correlation of the plotted functions in these two figures.
4. Comparison of frequency shift observed in simulation with analytic prediction.
5. Bursting behavior caused by single modes when kinetic drive is appreciably larger than damping rate, which is larger than the rate of plateau reconstitution.
6. (a) Experimental observation on TFTR showing that a near steady response to a TAE mode changes rapidly to another near steady level when icrf heating is turned off; (b) Simulation of this effect with threshold equation produces qualitatively similar results.
7. The formation of sidebands in time of several TAE modes in JET.
8. (a) Comparison of (a) mode amplitude vs. time between the JET experiment and threshold equation simulation.
(b) Snapshots of the calculated spectrum of the saturated mode (left) and the experimental spectrum (right).

9. Comparison of predicted saturation levels (solid curve) calculated by Nova K code using theory described in this work, with the results (circles) of a numerical simulation based on a hybrid δf -Monte-Carlo code (which accounts for particle collisions).
10. Effect of resonance overlapping. In (a) modes not overlap; there is local flattening but the general shape of inverted distribution is preserved. When modes overlap as in (b), the distribution completely flattens over all N modes, to produce roughly a factor N^2 more wave energy.
11. Correlation of particle loss with TAE bursts observed in a TFTR neutral beam experiment.

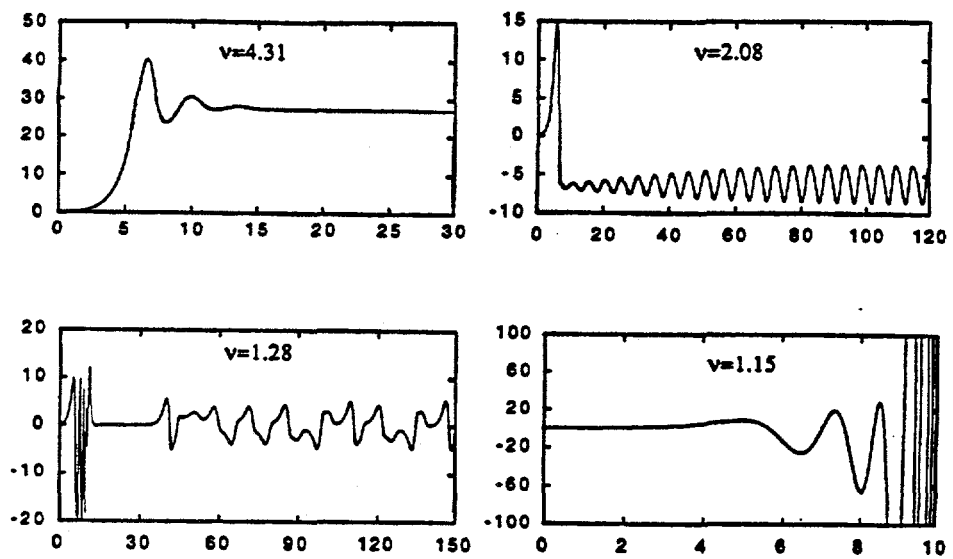


Fig 1.

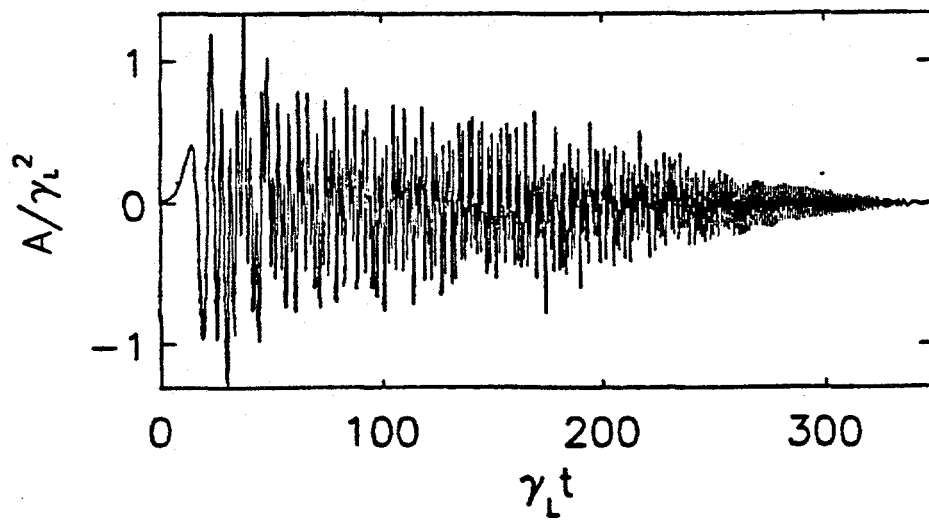
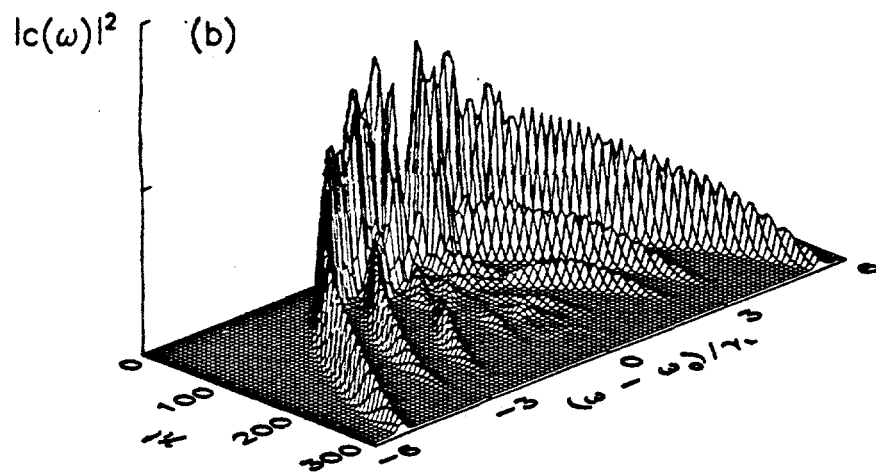
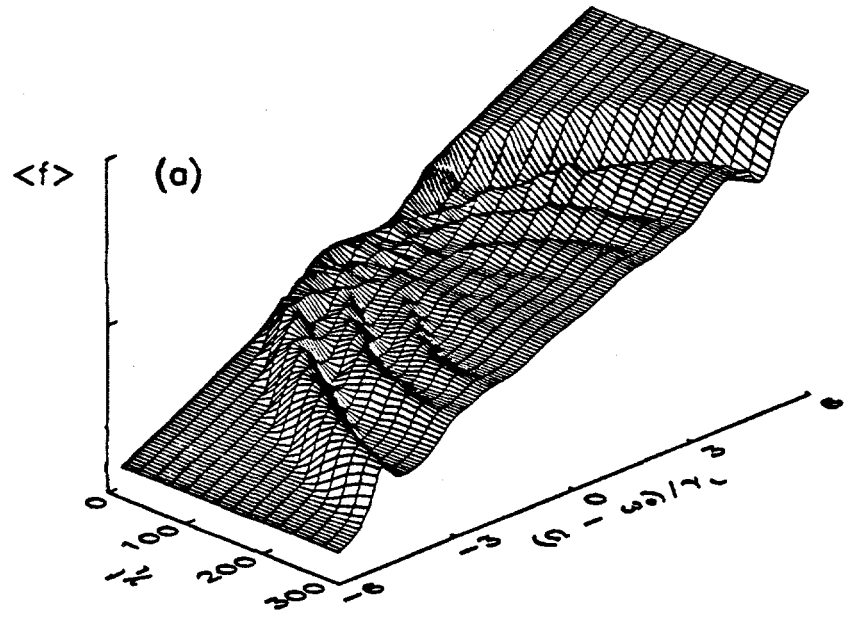


Fig 2.

Fig 3.



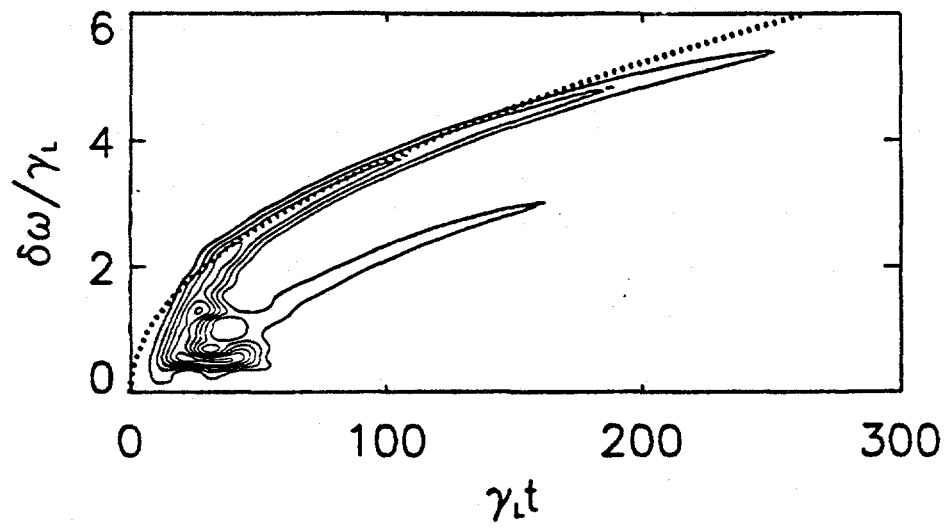


Fig 4.

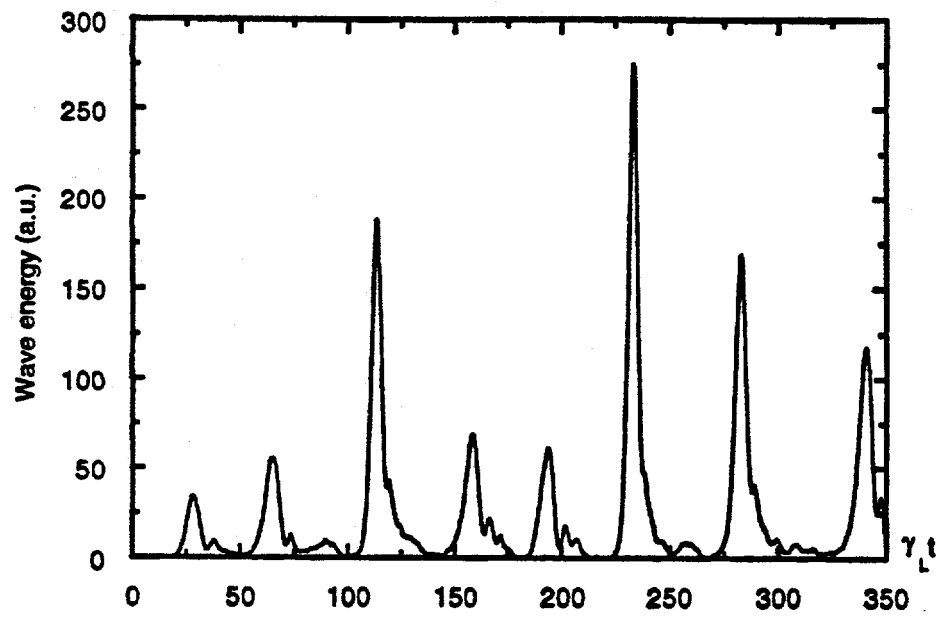


Fig 5.

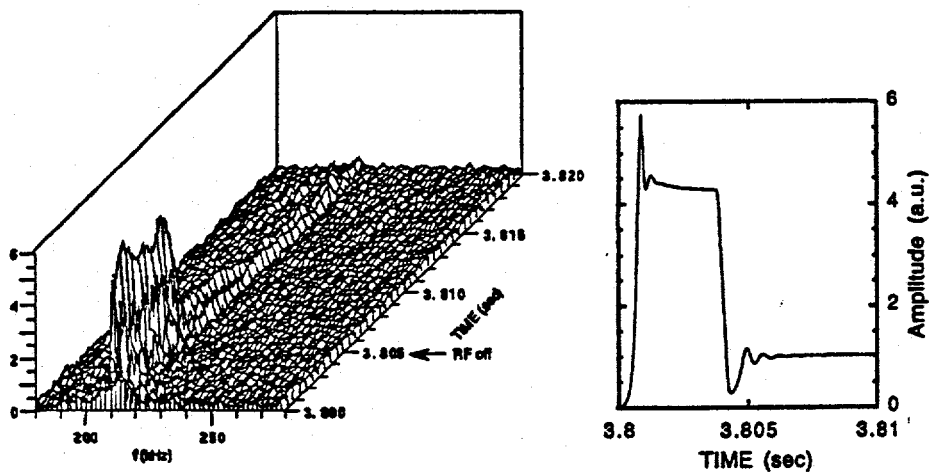


Fig 6.

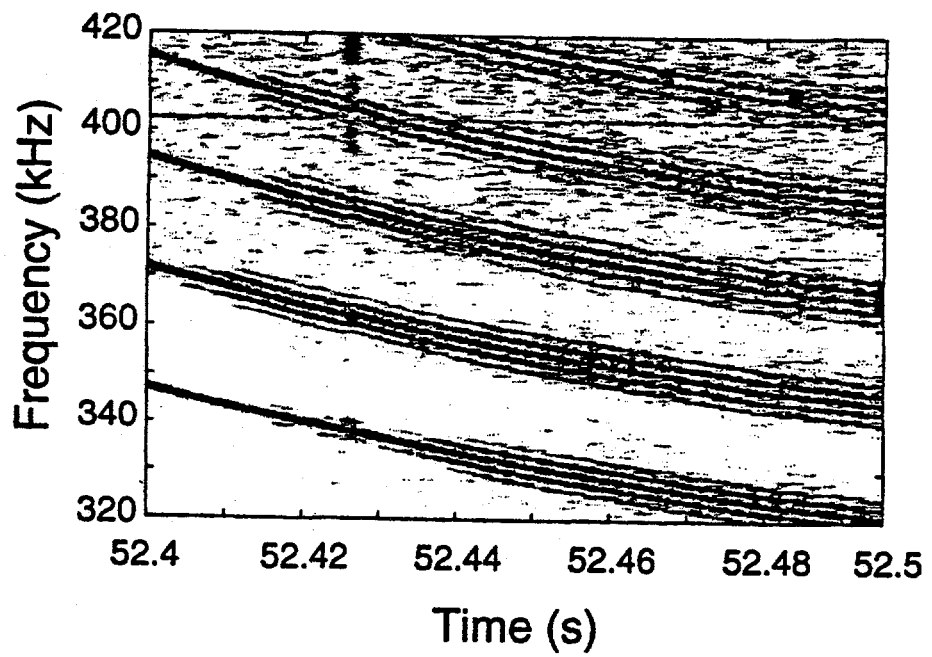


Fig 7.

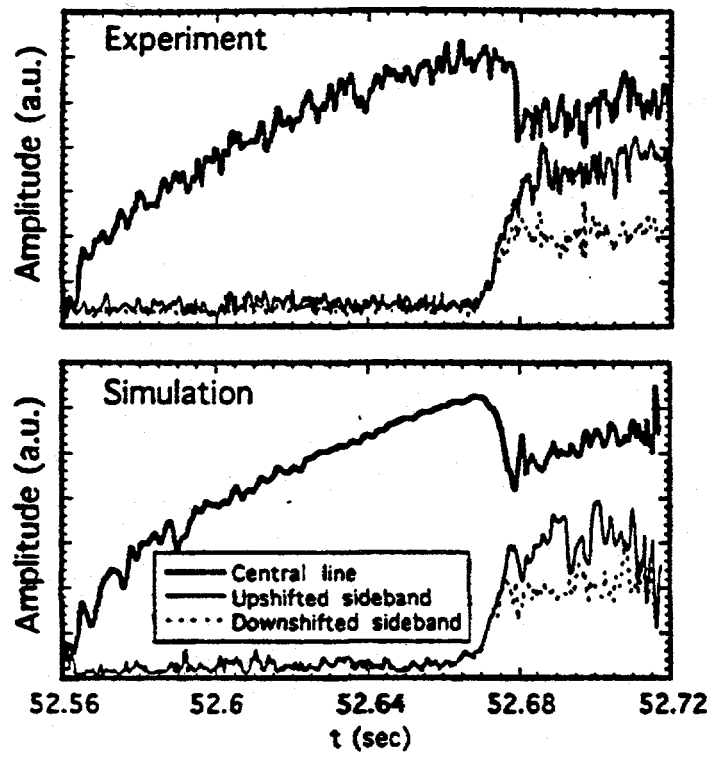


Fig 8a.

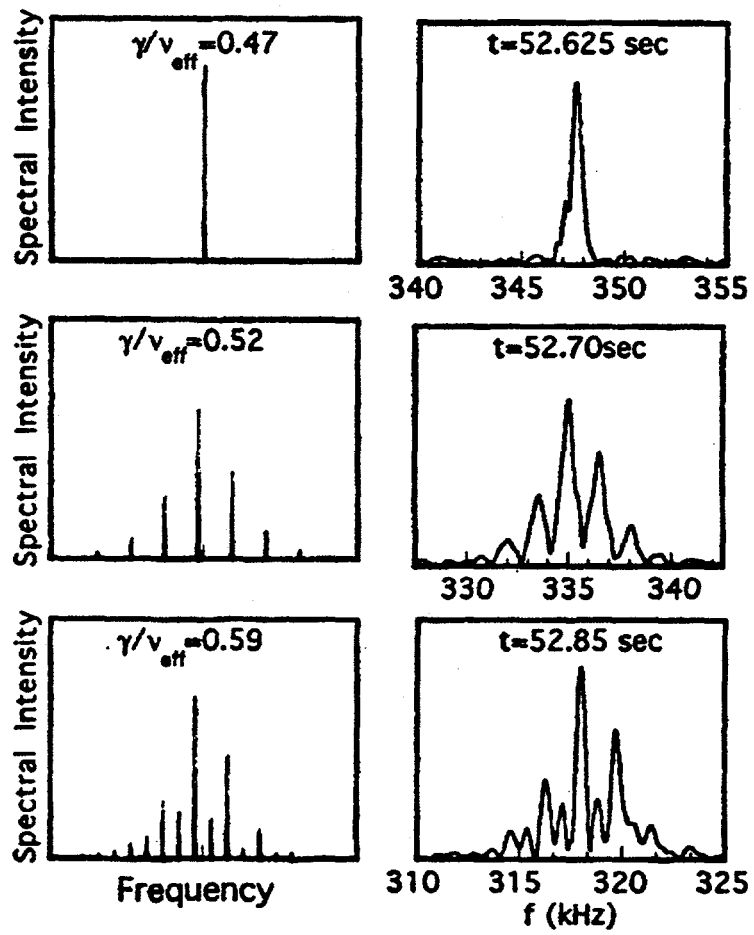


Fig 8b

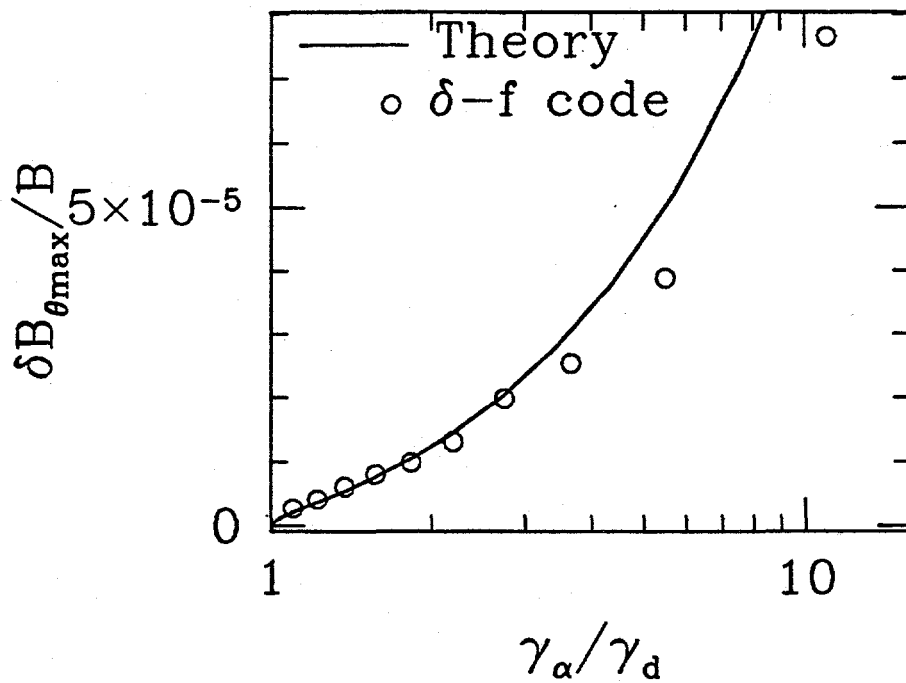
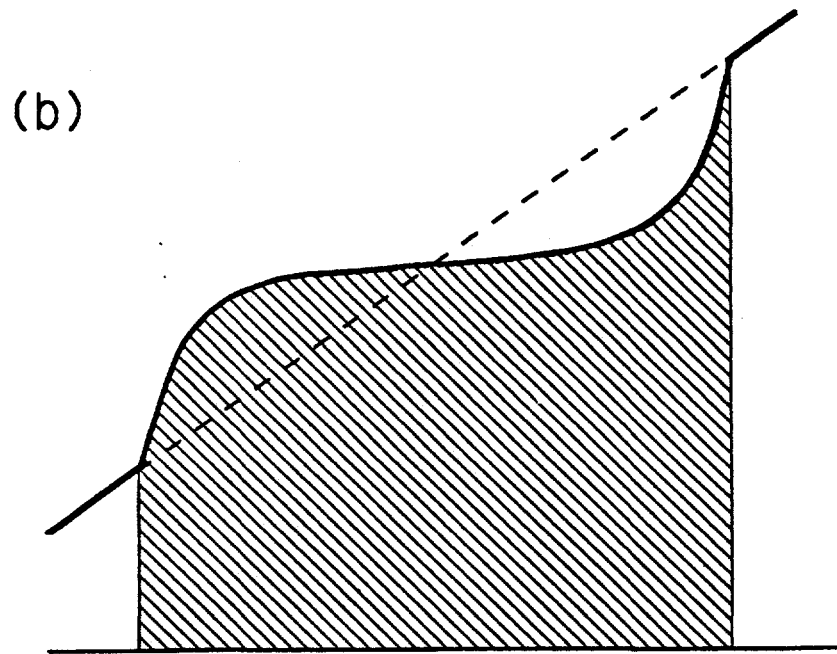
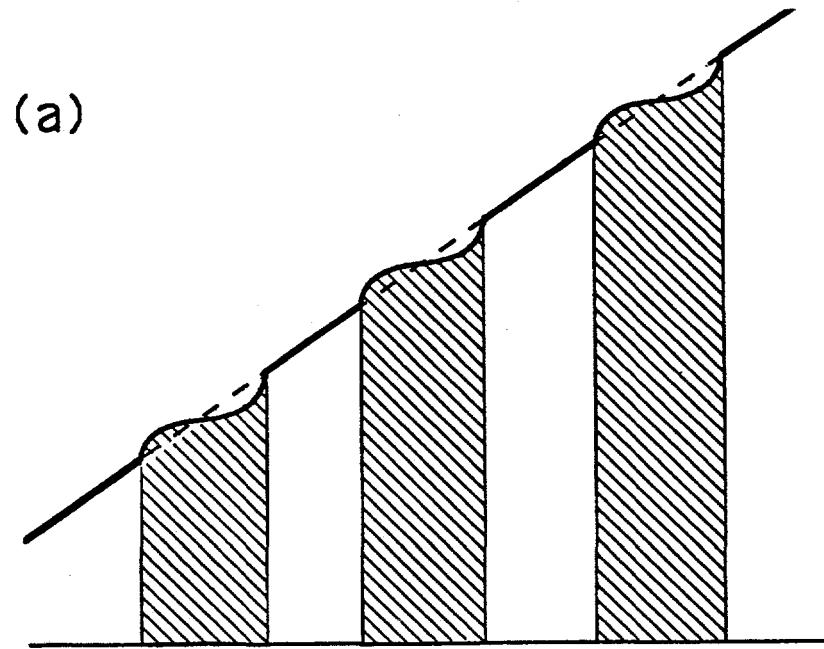


Fig 9.

Fig 10.



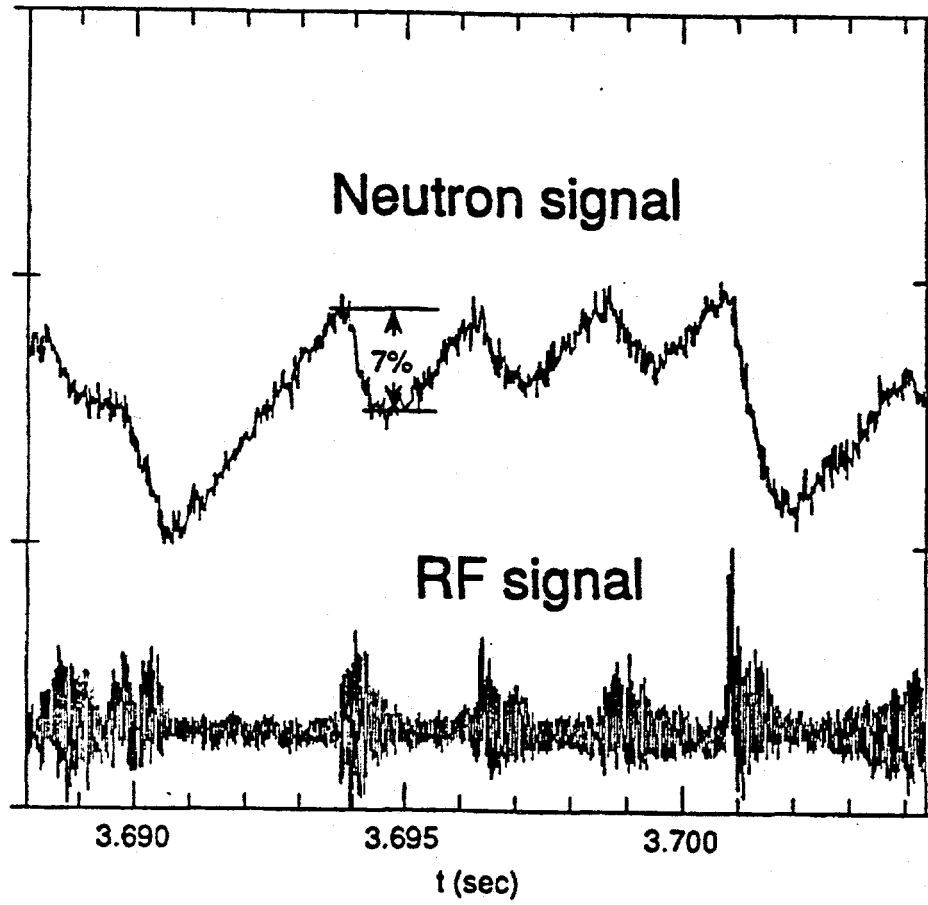


Fig 11.